Noninvasive mapping of spontaneous fluctuations in tumor oxygenation using ^{19}F MRI

J. Magat and B. F. Jordan
Biomedical Magnetic Resonance Unit, Louvain Drug Research Institute, Université Catholique de Louvain, Brussels 1200, Belgium

G. O. Cron
Magnetic Resonance Imaging, Ottawa Health Research Institute, Ottawa, Ontario K1S 5B6, Canada

B. Gallez[a]
Biomedical Magnetic Resonance Unit, Louvain Drug Research Institute, Université Catholique de Louvain, Brussels 1200, Belgium

Purpose: Acute hypoxia (transient cycles of hypoxia-reoxygenation) is known to occur in solid tumors and may be a poorly appreciated therapeutic problem as it can be associated with resistance to radiation therapy, impaired delivery of chemotherapeutic agents, or metastasis development. The objective of the present study was to use MR ^{19}F relaxometry maps to analyze the spontaneous fluctuations of partial pressure of oxygen (pO_2) over time in experimental tumors.

Methods: The pO_2 maps were generated after direct intratumoral administration of a fluorine compound (hexafluorobenzene) whose relaxation rate ($1/T_1$) is proportional to the % O_2. The authors used a SNAP inversion-recovery sequence at 4.7 T to acquire parametric images of the T_1 relaxation time with a high spatial and temporal resolution. Homemade routines were developed to perform regions of interest analysis, as well as pixel by pixel analysis of pO_2 over time.

Results: The authors were able to quantify and probe the heterogeneity of spontaneous fluctuations in tumor pO_2: (i) Spontaneous fluctuations in pO_2 occurred regardless of the basal oxygenation state (i.e., both in oxygenated and in hypoxic regions) and (ii) spontaneous fluctuations occurred at a rate of 1 cycle/12–47 min. For validation, the analysis was performed in dead mice for which acute changes did not occur. The authors thereby demonstrated that ^{19}F MRI technique is sensitive to acute change in pO_2 in tumors.

Conclusions: This is the first approach that allows quantitative minimally invasive measurement of the spontaneous fluctuations of tumor oxygenation using a look-locker approach (e.g., SNAP IR). This approach could be an important tool to characterize the phenomenon of tumor acute hypoxia, to understand its physiopathology, and to improve therapies. © *2010 American Association of Physicists in Medicine.* [DOI: 10.1118/1.3484056]

Key words: ^{19}F MRI, acute hypoxia, tumor oxygenation, pO_2 fluctuations

I. INTRODUCTION

Two types of hypoxia have been identified in tumors: Chronic hypoxia caused by an increase in diffusion distances between tumor vessels with tumor expansion and acute hypoxia caused by blood flow heterogeneities and temporally correlated with changes in red cell flux.[1,2] It is well known that acute hypoxia is associated with resistance to radiation therapy[3] and impaired delivery of chemotherapeutic agents.[4] Further studies have shown that intermittent hypoxia increases metastasis development[5] and promotes the survival of tumor cells.[6] Also, it has been recently shown that cycling through periods of acute hypoxia followed by reoxygenation will lead to an accumulation of unrepaired lesions and increased genomic instability.[7] Importantly, Rofstad *et al.*[8] demonstrated with immunochemistry that the fraction of acute hypoxic cells is larger than the fraction of chronic hypoxic cells. All these results emphasize the fact that the study

of acute hypoxia is of primary importance with regard to tumor development and cancer therapy and that there is a critical need for developing *in vivo* techniques to measure it with sufficient time and spatial resolutions.

In the past, acute changes over time have been characterized using multiple techniques: Intravital microscopy,[9–11] histologically based "mismatch" techniques,[12] and laser Doppler flowmetry.[13,14] Consecutively, both Eppendorf electrodes[15] and Oxylite fiberoptic probes[16,17] have been used to demonstrate transient changes in tumor oxygenation. In addition, the same group recently developed a first pass imaging microscopy technique in window chambers.[18] All these methods allowed to definitely establish the occurrence of acute hypoxia in solid experimental tumors but were either invasive, indirect, or limited by a lack of spatial information and/or real-time data acquisition.

Magnetic resonance imaging (MRI) has therefore been considered to noninvasively study periodic changes in tumor pressure of oxygen (pO_2). First, it was demonstrated that T_2^*

weighted gradient-echo MRI could be used to provide both temporal and detailed spatial information on spontaneous fluctuations of blood flow and/or oxygenation in tumor vasculature throughout the tumor.[19,20] A second method involving DCE-MRI was used by Brurberg *et al.*[21,22] to investigate blood flow fluctuations in tumors. Recently, using ^{18}F-FMISO PET, Wang *et al.*[23] identified acute changes in the intensity of the tracer in human tumors and, with a mathematical model, tried to separate acute from chronic hypoxia on images. Even though these studies were the first to probe noninvasively transient fluctuations of hemodynamic parameters, these techniques still did not provide any information on the real *absolute* pO$_2$ values changes over the tumor.

[19]F MRI oximetry[24] has been developed to quantify tissue pO$_2$ over time after intratumoral injection of a perfluorocarbon (FREDOM).[25–27] Indeed, Mason *et al.*[28,29] analyzed the distribution of tumor pO$_2$ in response to various inhaled gases thanks to the linear correlation between the relaxation rate of fluorine ($1/T_1$) and the pO$_2$.[30] In the paper of Le *et al.*,[31] they demonstrated that inhaled gas (100% O$_2$ challenge) induced a diverse response of specific tumor area (hypoxic and well-oxygenated). The method provides quantitative pO$_2$ measurements, with relatively good temporal and spatial resolutions.

The objective of the present study was to use a snapshot IR ^{19}F MRI method developed in our laboratory[32] to investigate pO$_2$ fluctuations in tumor over time in order to quantitatively estimate acute changes in tumor oxygenation. Jordan *et al.*[32] demonstrated that our technique is very sensitive to acute change of pO$_2$ with carbogen challenge. The snapshot method presents the unique advantage of a time resolution that is relevant for sampling acute hypoxia (1.5 min acquisition time), while keeping a similar spatial resolution that is reached with FREDOM. We first considered spontaneous changes in macroscopic tumor regions and then performed a pixel by pixel analysis of the evolution of pO$_2$ in order to create maps of transient changes in pO$_2$.

II. MATERIALS AND METHODS

II.A. Animals

Syngeneic transplantable mouse liver tumors[33] (TLTs) were injected intramuscularly in the thigh of 5 week-old male NMRI mice (Elevage Janvier, France). For inoculation, approximately 10^6 cells in 0.1 ml of media were injected intramuscularly into the right leg of the mice. Mice developed palpable tumors within a week of inoculation. Tumors were allowed to grow to 8 mm in diameter prior to experimentation. The animals were anesthetized by inhalation of isoflurane (induction: 2%; maintenance: 1.4%) delivered by a nose cone. We previously demonstrated that isoflurane anesthesia did not interfere with the occurrence of spontaneous fluctuations of oxygenation.[34] Hexafluorobenzene (HFB) was first deoxygenated by bubbling nitrogen during 5 min and injected directly into the tumor in the central and peripheral regions. Warm air was used to maintain mouse body temperature during MRI experiments. Experiments were performed on living as well as on dead mice (for control experiments).
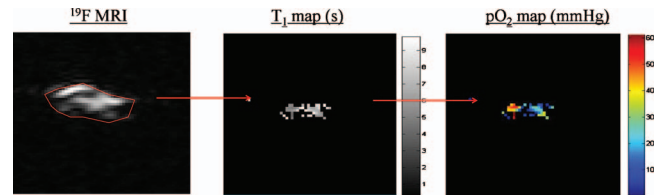
FIG. 1. Steps for ROI analysis: A ROI is selected on ^{19}F MRI images; a three-parameter fit is performed in each pixel to obtain T$_1$ map ($0 < T_1 < 10$s); and then, with the linear correlation between the rate of relaxation time and the partial oxygen, a pO$_2$ map is evaluated (pO$_2 > 0$ mm Hg).

II.B. MRI acquisition

Experiments were performed with a 4.7 T (200 MHz, ^{1}H) 40 cm inner diameter bore system (Bruker Biospec, Etlinger, Germany) with a tunable ^{1}H/^{19}F surface coil for transmission and reception. MRI scout images were obtained for both [1]H (200.1 MHz) and [19]F (188.3 MHz) to reveal HFB distribution within the tumor. We used a snapshot inversion recovery[32] (SNAP IR) sequence to acquire parametric images of T$_1$ relaxation time.[35,36] The sequence consisted of a nonselective hyperbolic secant inversion pulse (10 ms length), followed by acquisition of a series of 512 rapid gradient echo images. The parameters of the sequence were: Repetition time=10.9 ms, echo time=4.2 ms, flip angle =1°, field of view=60×30 mm, matrix=32×16, spectral width=12.5 kHz, and single thick slice (projection). Data were zero-filled to obtain a matrix with 64×64 pixels. Inversion times (TI) were in the range of TI$_1$=0.0932s to TI$_{512}$=89.2116s. The spatial resolution of the image is 1.88 mm and the temporal resolution is about 1.5 min without reconstruction of images. Acquisitions were performed during at least 1 h for living mice (a scan every 3 min) and during more than 2 h for dead mice (a scan every 5 min).

II.C. Data treatment

Home made routines were developed in MATLAB (The MathWorks, Inc., Natick, MA) to analyze ^{19}F MRI images:

II.C.1. Region of interest evolution (Figure 1)

For each MR image, we created a polygonal region of interest (ROI). A nonlinear fit was used to determine the T$_1$ relaxation in each pixel of the ROI (a three-parameter fit was performed on the signal intensity during inversion time using the standard inversion-recovery equation). A T$_1$ map was created (Fig. 1).

The calibration curve between R_1 ($R_1 = 1/T_1$) and the pO$_2$ was estimated in previous work on *in vitro* samples at 4.7 T and 37 °C.[32]
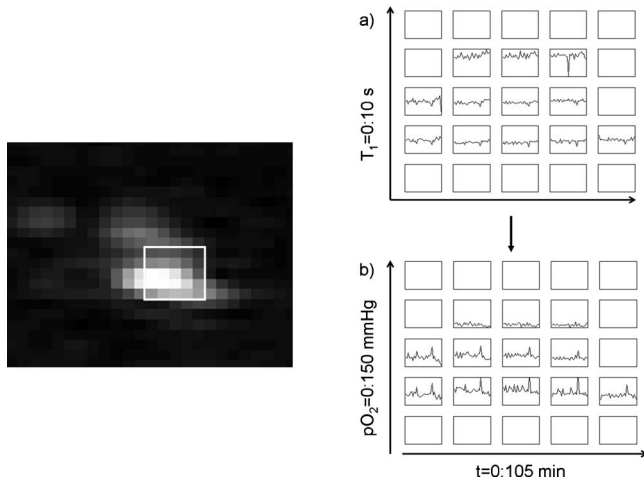
FIG. 2. Steps for pixel analysis: A rectangular ROI is selected in ^{19}F MRI images, pixels with a S/N ratio below 3 are removed, then (a) a three-parameter fit is performed to obtain T_1 evolution for each pixel and (b) the linear correlation between the rate of relaxation time and the partial oxygen a pO$_2$ map is evaluated (pO$_2 > 0$) for each pixel.

$$\text{pO}_2(\text{mm Hg}) = \frac{R_1(\text{s}^{-1}) - 0.1048}{0.002}. \tag{1}$$

We used the correlation between T_1 (s) and pO$_2$ (mm Hg) to obtain a map of the partial oxygen pressure. Then we analyzed the averaged pO$_2$ in several areas (ROIs) of the pO$_2$ maps. We estimated that pO$_2$ values had to be less than 500 mm Hg (these pixels censored represent only 0.1% of the data in the processing part).

II.C.2. Pixel evolution (Figure 2)

First, a rectangular ROI was defined on the images and the signal to noise ratio (S/N ratio) of fluorine was followed over time in each voxel of the ROI. The first step was to eliminate voxels with S/N inferior to 3 to get reliable pO$_2$ values, since we estimated that under this threshold, the pixel intensity was too noisy. The second step was to make a fit to

determine the relaxation time T_1 in each voxel, considering that the time T_1 has to be positive and inferior to 10 s [due to Eq. (1)]. And, finally, pO$_2$ values were analyzed over time for each pixel. Acceptable pixels had S/N ratio and T_1 above the thresholds (Fig. 2).

We used in the following text the terms "hypoxic" and "well-oxygenated" for a pO$_2$ below 10 mm Hg and for a pO$_2$ superior to 10 mm Hg as described in the literature.[1,5,22]

II.C.3. Fourier analysis of pO$_2$ fluctuations

Frequencies of pO$_2$ fluctuations were analyzed using the Fourier transform (fast Fourier transform algorithm). Frequency spectra are presented in power of pO$_2$ normalized by the maximum value. The frequency range was given by the acquisition sampling and the length of the experiment. For a living mouse, frequencies calculated were included between 0.22 and 2.7 mHz. For a dead mouse, the lowest and highest frequencies were 0.077 and 1.6 mHz, respectively.

II.C.4. Statistical analysis

Statistical analysis was performed using JMP 8 software (SAS, Cary, NC), where applicable, mean values of the different groups were compared using analysis of variance followed by *post hoc* Tukey–Kramer test for multiple comparisons. The significance level (α) was set to 0.05.

III. RESULTS

III.A. ROI analysis

Figure 3 represents a typical ROI analysis. A pO$_2$ map, overlaid on anatomical tumor image, has been generated showing different areas with regard to fluorine signal, in which four ROIs have been chosen to analyze the evolution of pO$_2$. We can see that pO$_2$ is fluctuating over time in all different areas. For ROIs 1 and 4, the pO$_2$ oscillates around (54.8 ± 3.6) and (46.7 ± 2.1) mm Hg, respectively (p=0.05, no significantly difference), corresponding to well-
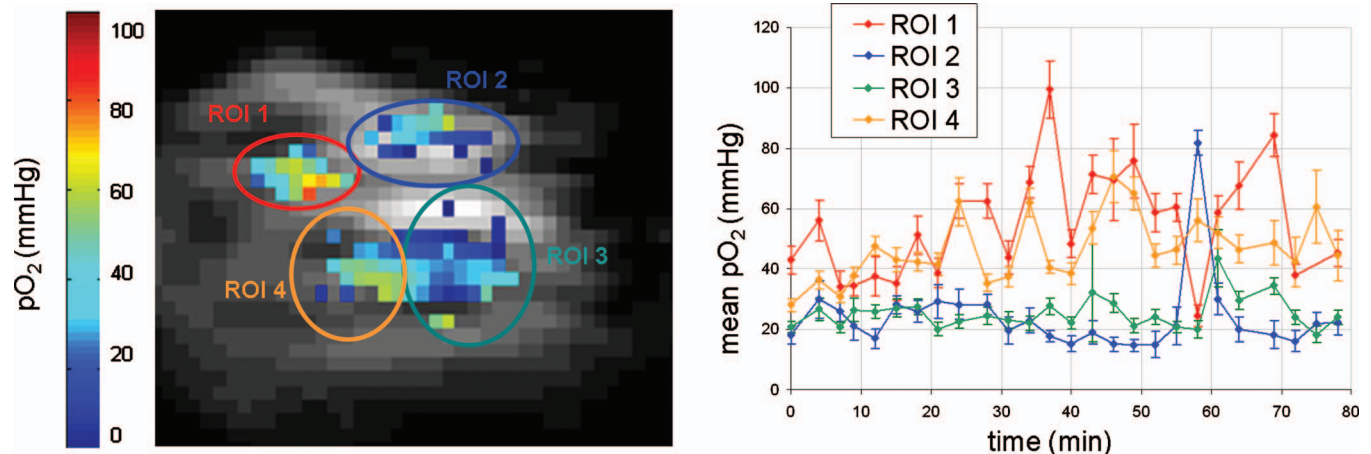
FIG. 3. Results obtained for a ROI analysis: The image represents the pO$_2$ map overlaid on anatomical tumor image (^{1}H MRI) in mm Hg (color bar between 0 and 100 mm Hg) with different ROIs. The graphic shows the mean pO$_2$ evolution during 80 min for each ROI.
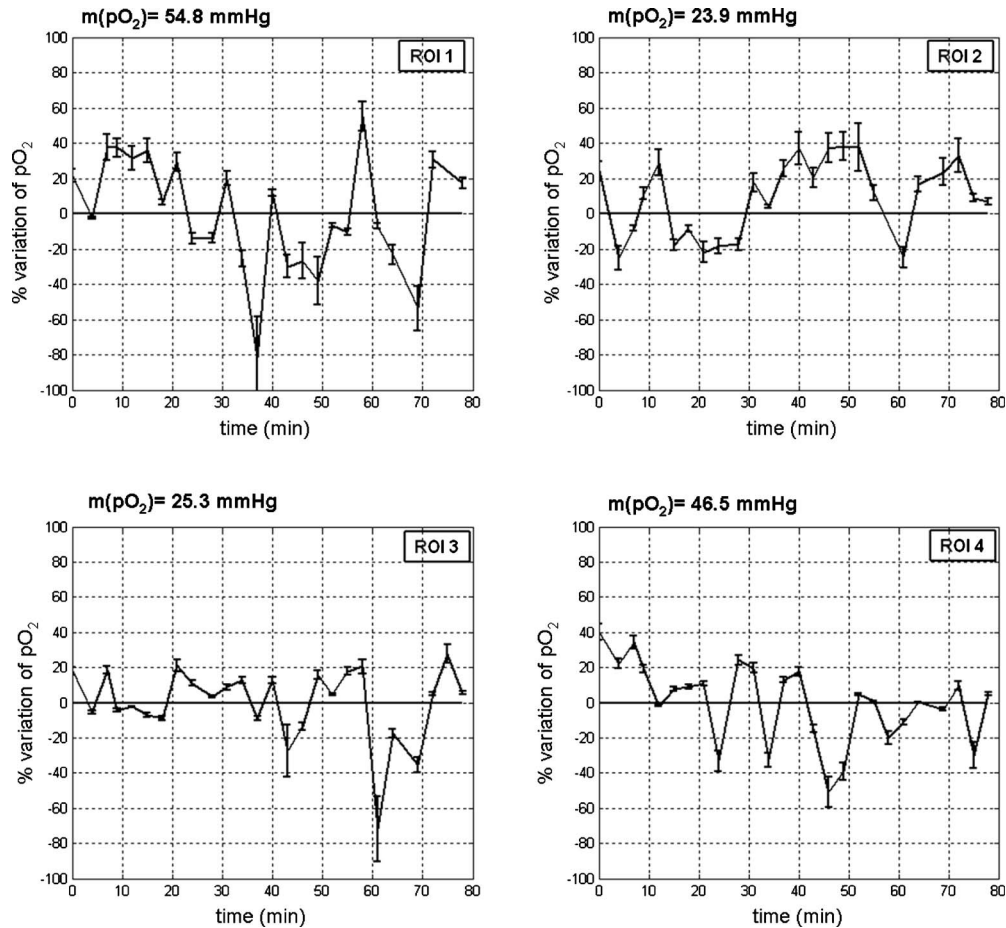
FIG. 4. Results obtained for a ROI analysis: The graphics represent the relative change of pO$_2$ in percentage in relation of pO$_2$ mean for each area.

oxygenated regions, whereas ROIs 2 and 3 correspond to less oxygenated regions, with a mean pO$_2$ around (23.9 ± 2.5) and (25.3 ± 1.0) mm Hg, respectively ($p = 0.99$, no significantly difference). The difference between ROI 1 and ROI 4, and ROI 2 and ROI 3 was statistically significant ($p < 0.001$, Tukey–Kramer).

The relative change in pO$_2$ (expressed in percentage of pO$_2$ variations reported to mean pO$_2$ for each area) is illustrated in Fig. 4: In ROIs 1 and 2, corresponding to a high and a low pO$_2$, respectively, in absolute value, more than half of the acquisitions have a pO$_2$ variation above 20% (which corresponds to the total absolute mean of relative change in pO$_2$). In comparison, in ROIs 3 and 4, most of the acquisitions have absolute relative pO$_2$ changes below 20%. The extent of fluctuations appears not to be related to the basal pO$_2$. Spontaneous fluctuations in pO$_2$ therefore occurred in all regions, regardless of the basal level of oxygenation.

III.B. Pixel analysis

A spatial study was performed by following the signal evolution in each pixel (1.88 mm) over time (for 215 min). Figure 5 shows typical results obtained on living and dead mice using an arbitrary ROI in the tumor. After data process-

ing, fluorine maps superimposed on the tumor anatomical proton image were generated and their respective pO$_2$ evolutions were evaluated (Figs. 5 and 6).

In living mice, after S/N ratio thresholding (arbitrary value of 3) and T$_1$ limitations, we obtained graphics of cyclic changes of pO$_2$ over time. We performed the data treatment in the entire tumor and the study revealed two types of relevant pixels already defined in Sec. II: Hypoxic pixels with pO$_2$ values around (4.6 ± 0.5) mm Hg, and more unstable well-oxygenated pixels with fluctuations between 12 and 57 mm Hg [with a mean of (34 ± 2) mm Hg]. Globally, after 75 min of acquisition, 31% of relevant pixels in all the tumor are hypoxic (< 10 mm Hg) and 69% of pixels represent a well-oxygenated area (> 10 mm Hg).

In the Fig. 5, 53% of pixels are not removed after selecting processing steps (S/N and T$_1$ threshold). The ROI revealed that 10% of pixels have a pO$_2$ between 4 and 10 mm Hg, 21% present a pO$_2$ between 10 and 20 mm Hg, and 69% are well-oxygenated with a mean of pO$_2$ above 20 mm Hg; several adjacent pixels have a high pO$_2$. With hypoxic pixels the information is more local; it has been observed that we can identify spots of hypoxia. This is shown in Fig. 5(b) that is based on the same data set as for the ROI analysis.
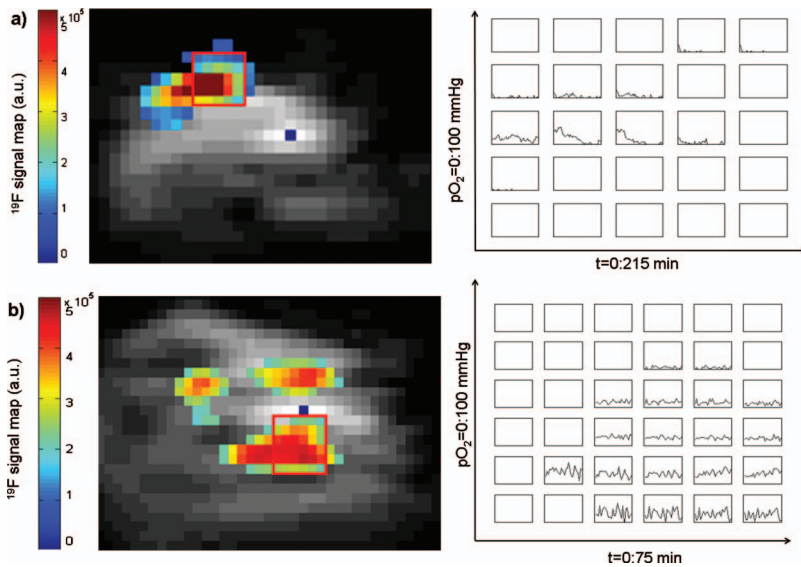
FIG. 5. Results obtained for a pixel analysis: Squares ROI were selected on fluorine MRI images superimposed on anatomical images (color bar between 0 and 5×10^5 a.u. ^{19}F MRI intensity). (a) Results for a dead mouse are presented with $0 < pO_2 < 100$ mm Hg during 215 min. (b) Results for a living mouse with $0 < pO_2 < 100$ mm Hg during 75 min. For each square, the y axis represents pO_2 between 0 and 100 mm Hg and the x axis is the time between 0 and 75 min.

A different pattern was observed after sacrifice [control mice in Fig. 5(a)], where a continuous decrease in pO_2 was identified during 2 h, resulting in only few pixels called "dead pixels" (only 40% of pixels are removed after data treatment in this ROI). The remaining pixels corresponded to pO_2 values that progressively went down to zero. No fluctuations were observed in postmortem data, contrarily to liv-ing data; which means that the fluctuations observed in healthy mice are not due to scanner instabilities.

III.C. Fourier transform of pixel analysis (frequency of fluctuations)

Figure 6 presents characteristic pO_2 fluctuations [Fig. 6(a)] and the Fourier spectra [Fig. 6(b)] corresponding to
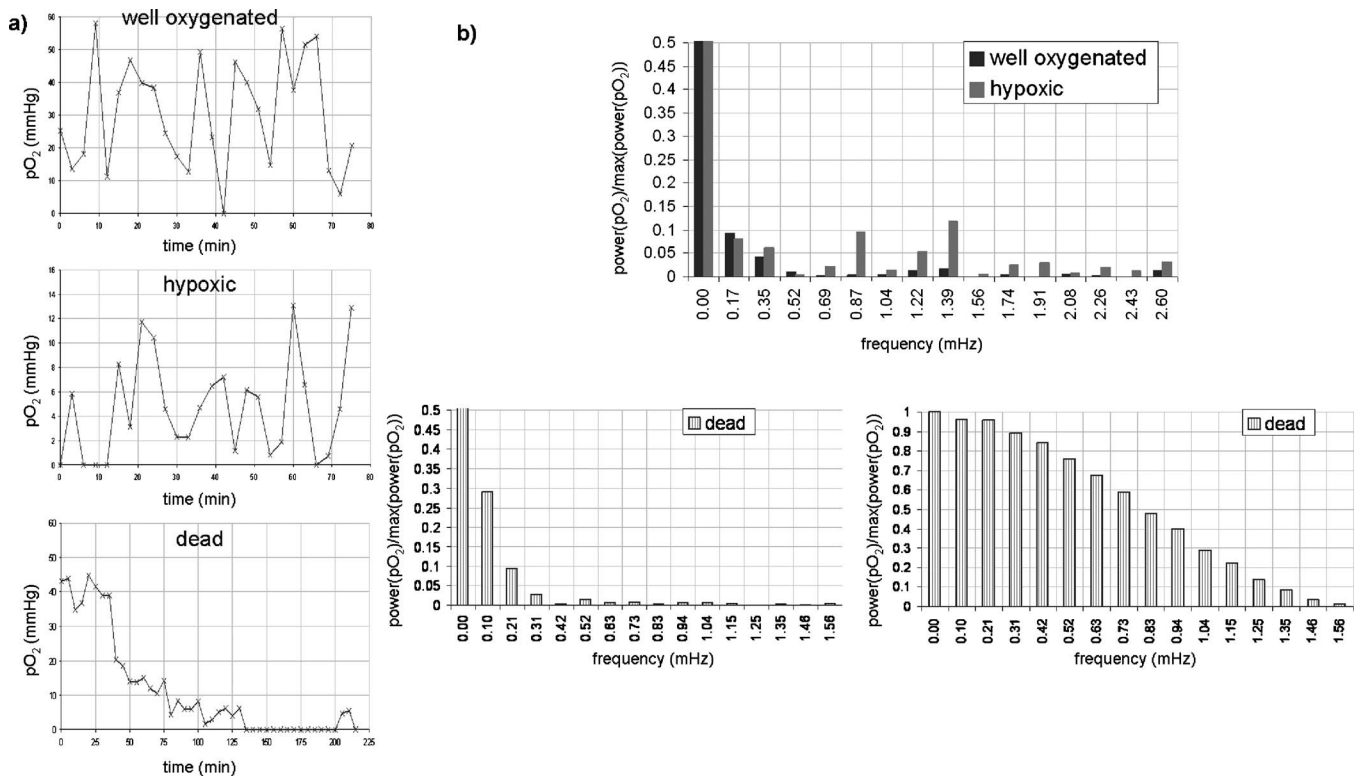
FIG. 6. Characteristic Fourier analysis of pO_2 fluctuations. (a) pO_2 variations over time for a well-oxygenated (mean of pO_2 around 30.3 ± 3.3 mm Hg), a hypoxic (mean of pO_2 around 4.6 ± 0.8 mm Hg), and a dead pixel (drop of pO_2), which occurs in a pixel analysis. (b) Fourier transforms corresponding to each pixel behavior for a living mouse (frequency range between 0 and 2.60 mHz) and for a dead mouse (frequency between 0 and 1.56 mHz). For a dead mouse, two spectra are presented: On the right, the Fourier analysis between 0 and 130 min and on the left, the Fourier analysis performed between 135 and 215 min.

TABLE I. Summary of techniques used to characterize acute hypoxia in tumors: Spatial resolution, temporal resolution, and some characteristics of the methods are presented.

Techniques	Spatial resolution	Temporal resolution	Characteristics
Eppendorf electrodes[a]	Tip diameter: 10 μm, 60–100 μm around tip	Sampling; 0.04 s	Local information; quantitative pO_2; invasive
Oxylite[b]	Tip diameter: 200–400 μm	5 s	Local information; quantitative pO_2; invasive
Window chamber[c]	10.8×10.8 μm^2 vessels: 0.67×0.67 μm^2	Nine images per second; 0.11 s	Flow measurement; invasive
T_2^* w GE-MRI[d]	470×470 μm^2	12.8 s	Signal intensity variation; noninvasive
DCE-MRI[c]	0.5×0.2 2 mm^3	15 min	Flow variation; noninvasive
^{18}F-FMISO PET[e]	4.2 mm	Days 1, 2, and 5	Tracer intensity variation; model interpretation; noninvasive
^{19}F MRI SNAP IR (this study)	1.88 mm	1.5 min	Noninvasive; quantitative pO_2

[a]Reference 34.
[b]References 15, 16, and 29.
[c]Reference 20.
[d]Reference 18.
[e]Reference 22.

hypoxic, well-oxygenated, and dead pixels which have been described in pixel analysis (see previous paragraph).

The first spectrum shows that all the activity in a well-oxygenated pixel (mean pO_2 around 30.3 ± 3.3 mm Hg) occurs below 0.35 mHz or 1 cycle/47 min. For the hypoxic pixel (mean pO_2 around 4.6 ± 0.8 mm Hg), pO_2 fluctuates at a frequency lower than 1 cycle/12 min, and the spectrum reveals two peaks: At 1.39 and 0.87 mHz or 1 cycle/12–20 min, respectively.

Fourier analysis for a dead pixel was split into two data treatments: A first frequency analysis was performed during 130 min and then a second Fourier transform is applied between 132 and 215 min. For the first analysis we can see that fluctuations are very slow with major frequencies below 0.31 mHz (1 cycle/54 min). For the second analysis, a large spectrum is observed and no characteristic frequencies are meaningful.

IV. DISCUSSION

The present study demonstrates that the ^{19}F MRI technique is sensitive to acute changes in pO_2 and reveals spontaneous pO_2 fluctuations in tumors over time, with the unique feature of being directly related to quantitative values of pO_2.

Spatial and temporal resolution and degree of invasiveness are important parameters to investigate spontaneous changes of pO_2 in the tumor (see comparison of techniques in Table I). Using the polarographic electrodes, Dewhirst *et al.*[37] demonstrated the phenomenon of spontaneous fluctuations at a microregional level. The technique has a good temporal resolution (frequency sampling of 25 Hz) and provides evidence for transient changes in pO_2. Nevertheless, the main limitation of this technique remains the restriction to a single point at a time measurement in each tumor, which is also the case for the consecutive studies using the Oxylite fiber-optic oxygen-sensing probe.[16,17] The window chamber method combined with microscopy for blood flow study in the tumor presents high spatial (vessel investigation) and temporal (video acquisition) resolution, but the technique is very invasive and cannot provide quantitative information on pO_2. In comparison with the ^{19}F MRI technique, these techniques have a very high temporal resolution (order of second) but they are invasive and suffer of lack of spatial distribution.

Our group further studied acute hypoxia in experimental tumors using T_2^* weighted MRI,[19,20] in which we could qualitatively correlate relative changes in signal intensity with fluctuation of pO_2. This technique acquired 140 scans during 30 min with a spatial resolution of 470 μm; unfortunately, the data could not be quantitatively related to the actual partial oxygen pressure.

More recently, Brurberg *et al.*[21] studied microenvironmental parameters using DCE-MRI with Kety analysis to determine blood perfusion in tumors. The DCE method involved a total acquisition time of 15 min with a voxel size about 0.2 mm.[4] Therefore, fluctuations occurring at a higher frequency range were not detected. With PET technique, Wang *et al.*[23] quantified acute and chronic hypoxia in the tumor with a mathematical model, but the measurement was performed once per day which is rather long for an oxygen dynamic study. ^{19}F MRI does not provide the best spatial resolution in comparison with other noninvasive methods, but it gives quantitative information of pO_2 over time with a temporal resolution consistent with the FREDOM method developed by Mason *et al.*[32,38]

^{19}F MRI oximetry with IR snapshot recovery is a reliable method able to provide quantitative and direct pO_2 information in the same area/pixel over time in the tumor with sufficient temporal (1.5 min) and spatial resolutions (1.88 mm) with regard to acute hypoxia.

In a first global analysis of different ROIs, it was shown that the pO_2 is oscillating in different oxygenated regions. Hunjan *et al.*[38] have also found heterogeneities in the distribution of pO_2 in tumors with poorly and well-oxygenated regions, using ^{19}F MRI acquisitions. Furthermore, by combining DCE-MRI technique with Oxylite measurement,

Brurberg *et al.*[22] showed that pO_2 transient changes were similar between poorly and well-oxygenated regions. pO_2 fluctuations were not affected by the mean basal pO_2. These results are consistent with our observed fluctuations in each ROI (Fig. 4). Indeed, the pO_2 pattern of fluctuations did not differ in well-oxygenated and more hypoxic areas.

Regarding the pixel by pixel study, living mice showed fluctuating pO_2 in numerous pixels (more than 53% of pixels fluctuated in this ROI). Two types of pattern were observed: Very hypoxic pixels with fluctuations around 5 mm Hg and more oxygenated pixels with strong fluctuations around 30 mm Hg.

Fourier analysis in Fig. 6(b) revealed various spectra for the different patterns: For a well-oxygenated pixel the frequency analysis is more like the dead pixel at the beginning during the drop of pO_2 and no cyclic fluctuations of pO_2 have been estimated. Whereas for a hypoxic pixel, two frequencies, characteristic of transient and cyclic change in pO_2, can be observed and analyzed.

We know from our previous T_2^* study that these cyclic changes are not related to physiological noise such as cardiac or respiratory noise. Evaluated frequency range for these fluctuations occurring in tumors at 1 cycle/10–60 min with recessed-tip oxygen microelectrodes[14] and at 1 cycle/3–30min with T_2^* weighted MRI.[19] The frequencies observed here are quite slow in comparison with those of the physiological noise. Indeed cardiac and respiratory cycles occur at 300–400 and 50–60 cycles/min, respectively.[14] The low frequency of fluctuating pixels is consistent with the Fourier analysis of our data which has been evaluated in a range of 1 cycle/12–47 min for a living mouse in different ROIs [Fig. 6(b)].

The pO_2 evolution was different in live and postmortem experiments, confirming that the fluctuations were not due to scanner instabilities: Oxygen evolution for sacrificed mouse showed a decrease in pO_2 over time, with only few important fluctuating pixels, and after 2 h, pO_2 tended to zero with a cessation of fluctuations. We have to note that acquisitions have been made after the death of the mouse. Howe *et al.*[39] has reported an increase of T_2^* during the N2 breathing until dead. This change has been interpreted as vascular collapse postmortem. However, our results are consistent with observations accompanying regional or total global ischemia in perfused heart using ^{19}F MRI[40,41] and following a vascular targeting agent[42] in rat breast carcinoma.

Indeed, Zhao *et al.*,[42] after administration of CA4P, a vascular targeting agent which causes a shut down of tumor vascular, observed a decrease of pO_2 very similar of the drop observed in our study for a dead mouse. Those observations are consistent with the decline of signal observed with T_2^* weighted MRI method after death:[19] During the first 2 h, the death physiological effects, including rigidity and drop of temperature, affected the T_1 time and consequently the estimated pO_2. Similar factors are likely to be the cause of the lack of relevant pixels for postmortem data after signal processing using the ^{19}F MRI method.

While comparing macroscopic (ROI) and microscopic (pixel) analysis, we can see that the absolute pO_2 values are more accurate in the pixel by pixel analysis with regard to relevant radiobiologically values. With the ROI analysis, we obtained information of change in oxygenation in various areas in the tumor, whereas with the pixel by pixel treatment the processing was more accurate and acute hypoxia was investigated. This is due to different factors, including thresholding step in the analysis, as well as the fact that the mean pO_2 measured in the ROI analysis is highly influenced by potential very well-oxygenated isolated pixels. The contribution of such pixels would have a huge influence on the mean or median analysis of the ROI. The values obtained using the pixel analysis on the TLT are in accordance with previously used techniques, including EPR oximetry and fiber-optic probes.[32,43]

To conclude, ^{19}F MRI oximetry is therefore a robust tool to characterize quantitatively tumor acute hypoxia. This unique tool could be further used to understand its underlying mechanisms, to assess the efficacy of therapies targeting these transient changes in pO_2, as well as to identify potential regions of resistance within a tumor.

ACKNOWLEDGMENTS

[a] Author to whom correspondence should be addressed. Electronic mail: bernard.gallez@uclouvain.be; Telephone: 32 2 7647391; Fax: 32 2 7647390.

[1] H. Kimura, R. D. Braun, E. T. Ong, R. Hsu, T. W. Secomb, D. Papahadjopoulos, K. Hong, and M. W. Dewhirst, "Fluctuations in red cell flux in tumor microvessels can lead to transient hypoxia and reoxygenation in tumor parenchyma," Cancer Res. **56**, 5522–5528 (1996).

[2] M. W. Dewhirst, "Relationships between cycling hypoxia, HIF-1, angiogenesis and oxidative stress," Radiat. Res. **172**, 653–665 (2009).

[3] D. J. Chaplin, P. L. Olive, and R. E. Durand, "Intermittent blood flow in a murine tumor: Radiobiological effects," Cancer Res. **47**, 597–601 (1987).

[4] R. E. Durand, "Intermittent blood flow in solid tumors—An under appreciated source of drug resistance," Cancer Metastasis Rev. **20**, 57–61 (2001).

[5] R. A. Cairns, T. Kalliomaki, and R. P. Hill, "Acute (cyclic) hypoxia enhances spontaneous metastasis of KHT murine tumors," Cancer Res. **61**, 8903–8908 (2001).

[6] P. Martinive, F. Defresne, C. Bouzin, J. Saliez, F. Lair, V. Grégoire, C. Michiels, C. Dessy, and O. Feron, "Preconditioning of the tumor vasculature and tumor cells by intermittent hypoxia: Implications for anticancer therapies," Cancer Res. **66**, 11736–11744 (2006).

[7] I. M. Pires, Z. Bencokova, M. Milani, L. K. Folkes, M. R. Stratford, A. L. Harris, and E. M. Hammond, "Effects of acute versus chronic hypoxia on DNA damage responses and genomic instability," Cancer Res. **70**, 925–935 (2010).

[8] E. K. Rofstad, K. Galappathi, B. Mathiesen, and E. B. M. Ruud, "Fluctuating and diffusion-limited hypoxia in hypoxia-induced metastasis," Clin. Cancer Res. **13**, 1971–1978 (2007).

[9] M. Intaglietta, R. R. Myers, J. F. Gross, and H. S. Reinhold, "Dynamics of microvascular flow in implanted mouse mammary tumours," Bibl. Anat. **15**, 273–276 (1977).

[10] M. W. Dewhirst, H. Kimura, S. W. Rehmus, R. D. Braun, D. Papahadjopoulos, K. Hong, and T. W. Secomb, "Microvascular studies on the origins of perfusion-limited hypoxia," Br. J. Cancer Suppl. **27**, 247–251

(1996).

[11]R. K. Jain, L. L. Munn, and D. Fukumura, "Dissecting tumour pathophysiology using intravital microscopy," Nat. Rev. Cancer **2**, 266–276 (2002).

[12]M. J. Trotter, D. J. Chaplin, R. E. Durand, and P. L. Olive, "The use of fluorescence probes to identify regions of transient perfusion in murine tumors," Int. J. Radiat. Oncol., Biol., Phys. **16**, 931–934 (1989).

[13]D. J. Chaplin and S. A. Hill, "Temporal heterogeneity at microregional erythrocyte flux in experimental solid tumours," Br. J. Cancer **71**, 1210–1213 (1995).

[14]R. D. Braun, J. L. Lanzen, and M. W. Dewhirst, "Fourier analysis of fluctuations of oxygen tension and blood flow in R3230Ac tumors and muscle in rats," Am. J. Physiol. Heart Circ. Physiol. **277**, 551–568 (1999).

[15]K. G. Brurberg, H. K. Skogmo, B. A. Graff, D. R. Olsen, and E. K. Rofstad, "Fluctuations in pO$_2$ in poorly and well-oxygenated spontaneous canine tumors before and during fractionated radiation therapy," Radiother. Oncol. **77**, 220–226 (2005).

[16]K. J. Brurberg, B. A. Graff, and E. K. Rofstad, "Temporal heterogeneity in oxygen tension in human melanoma xenografts," Br. J. Cancer **89**, 350–356 (2003).

[17]K. G. Brurberg, B. A. Graff, D. R. Olsen, and E. K. Rofstad, "Tumor-line specific pO$_2$ fluctuations in human melanoma xenograft," Int. J. Radiat. Oncol., Biol., Phys. **58**, 403–409 (2004).

[18]K. J. Brurberg, J. V. Gaustad, C. S. Mollatt, and E. K. Rofstad, "Temporal heterogeneity in blood supply in human tumor xenografts," Neoplasia **10**, 727–735 (2008).

[19]C. Baudelet, R. Ansiaux, B. F. Jordan, X. Havaux, B. Macq, and B. Gallez, "Physiological noise in murine solid tumours using T$_2^*$-weighted gradient-echo imaging: A marker of tumour acute hypoxia?," Phys. Med. Biol. **49**, 3389–3411 (2004).

[20]C. Baudelet, G. O. Cron, R. Ansiaux, N. Crokart, J. DeWever, O. Feron, and B. Gallez, "The role of vessel maturation and vessel functionality in spontaneous fluctuations of T$_2^*$—Weighted GRE signal within tumors," NMR Biomed. **19**, 69–76 (2006).

[21]K. J. Brurberg, I. C. Benjaminsen, L. M. R. Dorum, and E. K. Rofstad, "Fluctuations in tumor blood perfusion assessed by dynamic contrast-enhanced MRI," Magn. Reson. Med. **58**, 473–481 (2007).

[22]K. J. Brurberg, M. Thuen, E.-B. M. Ruud, and E. K. Rofstad, "Fluctuations in pO$_2$ in irradiated human melanoma xenografts," Radiat. Res. **165**, 16–25 (2006).

[23]K. Wang, E. Yorke, S. A. Nehmeh, J. L. Humm, and C. C. Ling, "Modeling acute and chronic hypoxia using serial images of ^{18}F-FMISO PET," Med. Phys. **36**, 4400–4408 (2009).

[24]D. Zhao, L. Jiang, and R. P. Mason, "Measuring changes in tumor oxygenation," Methods Enzymol. **386**, 378–418 (2004).

[25]R. P. Mason, W. Rodbumrung, and P. P. Antich, "Hexafluorobenzene: A sensitive 19F NMR indicator of tumor oxygenation," NMR Biomed. **9**, 125–134 (1996).

[26]S. P. Robinson and J. R. Griffiths, "Current issues in the utility of 19F nuclear magnetic methodologies for the assessment of tumor hypoxia," Philos. Trans. R. Soc. London, Ser. B **359**, 987–996 (2004).

[27]D. J. O. McIntyre, C. L. McCoy, and J. R. Griffiths, "Tumor oxygenation measurements by 19F MRI perfluorocarbons," Curr. Sci. **76**, 753–762 (1999).

[28]R. P. Mason, A. Constantinescu, S. Hunjan, D. Le, E. W. Hahn, P. P. Antich, C. Blum, and P. Peschke, "Regional tumor oxygenation and measurement of dynamics changes," Radiat. Res. **152**, 239–249 (1999).

[29]S. Hunjan, R. P. Mason, A. Constantinescu, P. Peschke, E. W. Hahn, and P. P. Antich, "Regional tumor oximetry: ^{19}F NMR spectroscopy of hexafluorobenzene," Int. J. Radiat. Oncol., Biol., Phys. **41**, 161–171 (1998).

[30]J.-J. Delpuech, M. A. Hamza, G. Serratice, and M.-J. Stébé, "Fluorocarbons as oxygen carriers. I. An NMR study of oxygen solutions in hexafluorobenzene," J. Chem. Phys. **70**, 2680–2687 (1979).

[31]D. Le, R. P. Mason, S. Hunjan, A. Constantinescu, B. R. Barker, and P. P. Antich, "Regional tumor oxygen dynamics: ^{19}F PBSR EPI of hexafluorobenzene," Magn. Reson. Imaging **15**, 971–981 (1997).

[32]B. F. Jordan, G. O. Cron, and B. Gallez, "Rapid monitoring of oxygenation by 19F magnetic resonance imaging: Simultaneous comparison with fluorescence quenching," Magn. Reson. Med. **61**, 634–638 (2009).

[33]H. Taper, G. W. Woolley, M. N. Teller, and M. P. Lardis, "A new transplantable mouse liver tumor of spontaneous origin," Cancer Res. **26**, 143–148 (1966).

[34]C. Baudelet and B. Gallez, "Effect of anesthesia on the signal intensity in tumors using BOLD-MRI: Comparison with flow measurements by laser Doppler flowmetry and oxygen measurements by luminescence-based probes," Magn. Reson. Imaging **22**, 905–912 (2004).

[35]S. Laukemper-Ostendorf, A. Scholz, K. Burger, C. P. Heussel, M. Schmittner, N. Weiler, K. Markstaller, B. Eberle, H.-U. Kauczor, M. Quintel, M. Thelen, and W. G. Schreiber, "19F MRI of perflubron for measurement of oxygen partial pressure in porcine lungs during partial liquid ventilation," Magn. Reson. Med. **47**, 82–89 (2002).

[36]S. Blüm, L. R. L. Schad, B. Stephanow, and W. J. Lorenz, "Spin-lattice relaxation time measurement by means of a TurboFLASH technique," Magn. Reson. Med. **30**, 289–295 (2002).

[37]M. W. Dewhirst, R. D. Braun, and J. L. Lanzen, "Temporal changes in pO$_2$ of R3230AC tumors in fisher-344 rats," Int. J. Radiat. Oncol., Biol., Phys. **42**, 723–726 (1998).

[38]S. Hunjan, D. Zhao, A. Constantinescu, E. W. Hahn, P. P. Antich, and R. P. Mason, "Tumor oximetry: Demonstration of an enhanced dynamic mapping procedure using fluorine-19 echo planar magnetic resonance imaging in the dunning prostate R3327-AT1 rat tumor," Int. J. Radiat. Oncol., Biol., Phys. **49**, 1097–1108 (2001).

[39]F. A. Howe, S. P. Robinson, D. J. McIntyre, M. Stubbs, and J. R. Griffiths, "Issues in flow and oxygenation dependent contrast (FLOOD) imaging of tumours," NMR Biomed. **14**, 497–506 (2001).

[40]H. P. Shukla, R. P. Mason, N. Bansal, and P. P. Antich, "Regional myocardial oxygen tension: 19F MRI of sequestered perfluorocarbon," Magn. Reson. Med. **35**, 827–833 (1996).

[41]J.-X. Yu, W. Cui, D. Zhao, and R. P. Mason, in *Fluorine and Health*, edited by A. Tressaud and G. Haufe (Elsevier, Amsterdam, 2008), pp. 198–276.

[42]D. Zhao, L. Jiang, E. W. Hahn, and R. P. Mason, "Tumor physiological response to combretastatin A4 phosphate assessed by MRI," Int. J. Radiat. Oncol., Biol., Phys. **62**, 872–880 (2005).

[43]C. Diepart, B. F. Jordan, and B. Gallez, "A new EPR oximetry protocol to estimate the tissue oxygen consumption in vivo," Radiat. Res. **172**, 220–225 (2009).